BMC Cancer

RESEARCH

Open Access

Added value of pretreatment CT-based Node-RADS score for predicting survival outcome of locally advanced gastric cancer: compared with clinical N stage

Yan Sun[1,2†], Lu Wen[1†], Wang Xiang[1], Xiangtong Luo[3], Lian Chen[1], Xiaohuang Yang[1], Yanhui Yang[1,2], Yi Zhang[1,2], Sanqiang Yu[4], Hua Xiao[5,6*] and Xiaoping Yu[1,2*]

Abstract

Objectives The Node Reporting and Data System (Node-RADS) offers a reliable framework for lymph node assessment, but its prognostic significance remains unexplored. This study aims to investigate the added prognostic value of Node-RADS in patients with locally advanced gastric cancer (LAGC) undergoing neoadjuvant chemotherapy (NAC) followed by gastrectomy.

Materials and methods This single-center retrospective study included 118 patients with LAGC underwent NAC and gastrectomy. The maximum Node-RADS score and the number of metastatic lymph node stations (defined as LNM-Station) were evaluated on pretreatment CT. The pretreatment Node-RADS-CT and Node-RADS-integrated models were developed using Cox regression to predict overall survival (OS) and disease-free survival (DFS). The pretreatment cN-CT models, cN-integrated models, as well as post-NAC pathological models were also developed in comparison. The performance of the models was assessed in terms of discrimination, calibration and clinical applicability.

Results The LNM-Station was significantly associated with OS and DFS (all $p < 0.05$). The Node-RADS-CT model showed higher Harrell's consistency index (C-index) than cN-CT model (0.755 vs. 0.693 for OS, $p = 0.017$; 0.759 vs. 0.706 for DFS, $p = 0.018$). The Node-RADS-integrated model also achieved higher C-index than cN-integrated model (0.771 vs. 0.731 for OS, $p = 0.091$; 0.773 vs. 0.733 for DFS, $p = 0.053$). The net reclassification improvement (NRI) of the Node-RADS-integrated model at 5 years was 0.379 for OS and 0.364 for DFS (all $p < 0.05$). The integrated discrimination improvement (IDI) of the Node-RADS-integrated model was 0.103 for OS and 0.107 for DFS (all $p < 0.05$). The C-indices

†Yan Sun and Lu Wen contributed equally to this work.

Xiaoping Yu and Hua Xiao are the co-corresponding authors of this article

*Correspondence:
Hua Xiao
xiaohua@hnca.org.cn
Xiaoping Yu
yuxiaoping@hnca.org.cn

Full list of author information is available at the end of the article

(OS: 0.745; DFS: 0.746) of pathological models were slightly lower than those of Node-RADS-based models (all $p > 0.05$).

Conclusion The baseline Node-RADS score and LNM-Station were effective prognostic indicators for LAGC. The pretreatment CT Node-RADS-based models can offer added prognostic value for LAGC, compared with clinical N stage.

Keywords Gastric cancer, Prognosis, Lymph node, Node-RADS, CT

Introduction

Gastric cancer is the fifth most commonly diagnosed cancer and the fifth leading cause of cancer-related mortality worldwide [1]. The majority of patients are diagnosed with locally advanced gastric cancer (LAGC), and the neoadjuvant chemotherapy (NAC) combined with radical surgery has brought survival benefit for LAGC patients [2–4]. Nonetheless, the survival outcome remains poor with a dismal 5-year overall survival (OS) rate of 31% and a high recurrence rate exceeding 60% [5, 6]. Recent studies proved that new kinds of adjuvant treatments, such as immunotherapy, heated intraperitoneal chemotherapy and radiotherapy, brought promising prognostic results [7–10]. Therefore, early and accurate survival prediction is crucial for identifying LAGC patients with poor outcomes, allowing for additional adjuvant therapy and more frequent follow-up.

The TNM staging system of American Joint Committee on Cancer is widely used for treatment selection and prognosis of LAGC [11, 12]. However, studies have shown that LAGC patients with same TNM stage and similar treatment regimens exhibit different survival outcomes [13, 14], suggesting that traditional TNM staging system is insufficient for providing personalized prognostic information.

The clinical N (cN) stage, based on the number of suspicious positive lymph nodes (LNs), has been demonstrated to be associated with survival outcome of LAGC [12, 15]. The current CT criteria for determining LNs metastasis include LN size, local convergence, and enhancement consistency with the primary lesion, with size being the primary basis [12]. However, both metastatic LNs and reactive hyperplastic LNs can present as enlarged nodes, with size criteria varying widely from 6 to 20 mm [16]. That is to say, one major factor encumbering cN staging is that it doesn't consider the prognostic value of the LN morphologic characteristics (such as enlargement, capsule invasion, necrosis). Studies have shown that the enlarged size, necrosis, spherical shape and irregular borders of LNs are related to worse survival outcomes in various malignancies [17–20]. Additionally, the number of LN stations involved has been repeatedly proven to be a supplementary stratification factor to N stage for prognosis in malignant tumor such as non-small cell lung cancer [21, 22]. However, the prognostic significance of these LN-related factors has not yet been well explored in gastric cancer patients.

Baseline contrast-enhanced CT scan is the recommended imaging method for the staging of LAGC prior to anti-tumor therapy, offering high spatial resolution at a relatively low cost. In 2021, the Node Reporting and Data System (Node-RADS) was developed to standardize the assessment of LNs in malignancies of any organ, based on CT/MRI imaging [23]. Node-RADS assigns a grading-score to evaluate the probable involvement of LNs, with scores ranging from 1 to 5, indicating malignancy likelihood from very low to very high. This system has enhanced diagnostic accuracy for assessing LNs in various cancers, including those of stomach, bladder, prostate, lung, colon, and cervix [16, 24–28]. Nevertheless, the relationship between Node-RADS and prognosis has not been well discussed.

Therefore, the present study aimed to investigate the prognostic value of pretreatment CT-based Node-RADS score in locally advanced gastric cancer, compared to the cN stage.

Materials and methods

This retrospective study was approved by the Ethics Committee of Hunan Cancer Hospital and written informed consent was waived.

Participants

A total of 155 consecutive patients with histopathologically confirmed gastric cancer who underwent NAC followed by radical gastrectomy at Hunan Cancer Hospital between April 2015 and June 2020 were initially considered for this study.

The inclusion criteria were: (a) pathologically proven LAGC; (b) classified as LAGC (cT2-4NxM0) according to the TNM staging system of AJCC; (c) underwent standard NAC followed by radical gastrectomy and D2 regional lymphadenectomy; and(d) underwent baseline contrast-enhanced abdominal CT within 1 week before NAC. The exclusion criteria are listed in the study flowchart in Fig. 1.

All the included patients (cT2-4NxM0) received standard NAC regimens recommended by National Comprehensive Cancer Network (NCCN) / Chinese Society of Clinical Oncology (CSCO) guidelines [29, 30], with

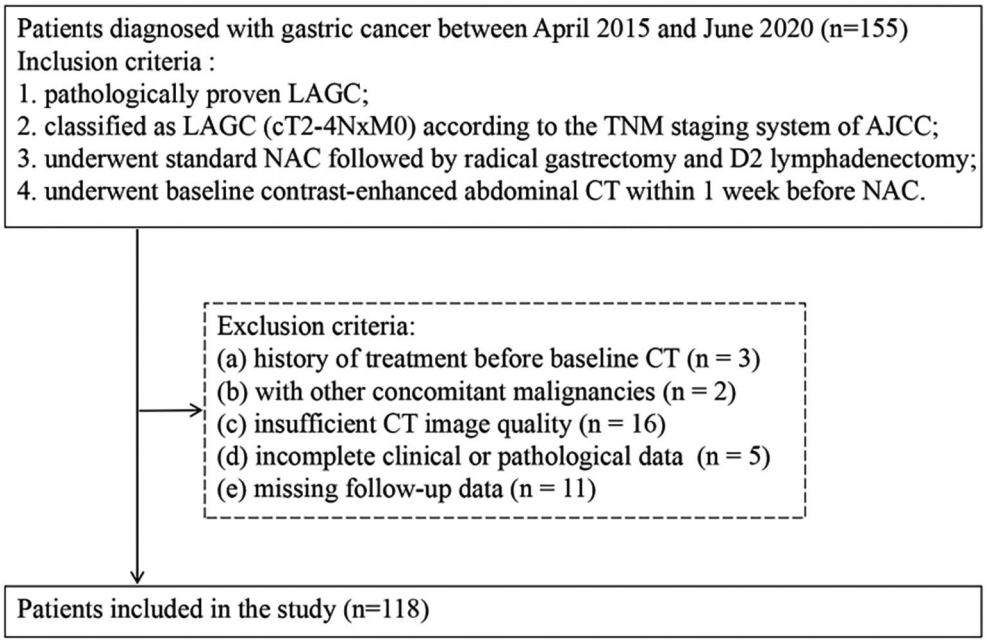

Fig. 1 Study flowchart

details in ESM (1). Clinical-pathologic and outcome data are shown in ESM (2). The lymph node ratio (LNR) was defined as the proportion of metastatic LNs to the total number of harvested LNs. The primary survival endpoint was OS, defined as the time from surgery to death from any cause. The secondary endpoint was disease-free survival (DFS), defined as the time from surgery to tumor recurrence or death from any cause.

CT examination and Node-RADS assessment

CT scanning scheme is introduced in ESM (3). Two radiologists experienced in abdominal CT imaging, Reader A (Y.S., 11 years) and Reader B (L.C., 23 years), separately assessed regional LNs on venous phase CT images before NAC, blinded to pathology and outcome data. Consensus was reached in the event of disagreement. The regional LNs were scored according to the Node-RADS system guided by the three-level flowchart (Fig.A.1). The Node-RADS defined LNs on size and configuration criteria with an overall score from 1 to 5 to indicate the likelihood of a nodal metastasis [23]. Examples of Node-RADS assessment are displayed in Fig. 2. LNs from regional stations (No.1–12) were evaluated separately and the highest score of all LNs was defined as the Node-RADS score at the patient level.

According to the Node-RADS reporting rules, scores of 4 and 5 should be reported as positive LN [23]. Moreover, Node-RADS scores of ≥ 4 and ≥ 3 exhibited similarly excellent performance in a previous study assessing LNs in gastric cancer, whereas a score of ≥ 4 demonstrated a higher specificity of 98.1% [16]. Therefore, we classified a score of ≥ 4 as indicative of a positive LN on CT, and accordingly LNM-Station was defined as the number of LN stations with at least one positive LN.

Statistical analysis

All data statistics were performed using SPSS 25.0 and R software (version 4.3.0) with a significance level of $p < 0.05$. Intraclass correlation coefficient (ICC) was employed to evaluate both intra-observer and inter-observer reliability of Node-RADS score.

Cutoff values for Node-RADS score, LNM-Station and cN stage to predict OS/DFS were determined using the receiver-operator characteristic (ROC) curve and maximum Youden's index. Kaplan-Meier curves and Cox proportional hazards regression were employed for survival analyses. Harrell's consistency index (C-index) was generated to assess the discriminative performance of the models. The *p*-value of C-index between different models was calculated, using the Z testing with R package 'CsChange'. Time-dependent ROC (Time-ROC) curves evaluated the accuracy of prognostic models at different time points. Net reclassification improvement (NRI) and integrated discrimination improvement (IDI) indices quantified the added prognostic value. Calibration curves assessed model calibration ability, and decision curve analysis (DCA) assessed clinical utility.

Results

Study demographics

A total of 118 patients (82 men and 36 women) were eventually included in the cohort, with the median

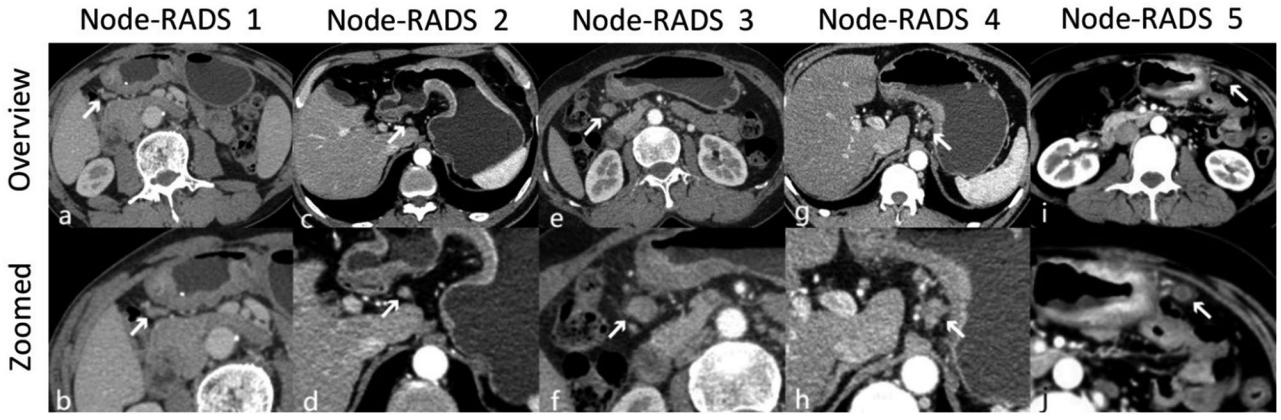

Fig. 2 Examples of Node-RADS scoring. Arrows point to the selected LNs. (**a**, **b**) Node-RADS 1. A 67-year-old male with cT4N0 GC. The selected LN in station No. 6 measures 12 × 5 mm with homogeneous texture, smooth border and oval shape. (**c**, **d**) Node-RADS 2. A 51-year-old male with cT2N0 GC. The selected LN in station No. 3 measures 7 × 7 mm with homogeneous texture, smooth border and spherical shape. (**e**, **f**) Node-RADS 3. A 53-year-old male with cT4N3 GC. The selected LN in station No. 6 measures 19 × 18 mm with homogeneous texture, smooth border and spherical shape. (**g**, **h**) Node-RADS 4. A 47-year-old female with cT2N2 GC. The selected LN in station No. 3 measures 17 × 13 mm with heterogeneous texture, irregular border and oval shape. (**i**, **j**) Node-RADS 5. A 45-year-old female with cT4N3 GC. The selected LN in station No. 4 measures 9 × 9 mm with gross necrosis, irregular border and spherical shape. LN, lymph node; Node-RADS, Node Reporting and Data System; GC, gastric cancer

age of 54 ± 11 years (Fig. 1). In terms of Lauren type, most LAGC tumors were classified as diffuse type (72[61.02%]), followed by mixed type (28[23.72%]) and intestinal type (18[15.25%]). 99(83.90%) patients were poorly differentiated or undifferentiated, 17(14.41%) were moderate differentiated and 2(1.69%) were well differentiated. There were 81(68.64%) patients in cT4, 25(21.19%) in cT3 and 12(10.17%) in cT2 stage.

The median follow-up time was 54 months (95%CI:49–65), with a median survival of 31 months. The clinicopathological characteristics of all included patients are detailed in Table 1.

Observer agreement for Node-RADS score

The inter-observer ICC of Node-RADS score for LNs at patient level was 0.796 (95%CI:0.737–0.854). Reader A reassessed the Node-RADS scores of all included patients three months after the initial assessment to obtain the intra-observer ICC. The intra-observer ICC of Node-RADS scores was 0.844(95%CI:0.775–0.891), reflecting a good consistency. The inter-observer and intra-observer ICC values of the Node-RADS score for LNs in stations No. 1–12 exceeded 0.717, as detailed in Table A.1.

Pretreatment Node-RADS Score and LNM-Station Associated with OS and DFS

In predicting OS/DFS, the cut-off value of LNM-Station was 2, Node-RADS score was 5, and cN stage was 3. Patients with fewer metastatic lymph node stations (0–1) exhibited significantly higher 5-year OS and DFS rates compared to those with multiple affected stations (> 2) (OS, 55.7% vs. 20.1%; DFS, 54.5% vs. 15.1%, both $p < 0.001$, Fig. 3a-b). The lower Node-RADS score (OS, 52.1% vs. 22.4%, $p = 0.002$; DFS, 57.0% vs. 20.3%, $p < 0.001$) and earlier cN stage (OS, 53.8% vs. 27.7%, $p = 0.004$; DFS, 55.4% vs. 16.8%, $p = 0.002$) were also related with higher 5-year OS and DFS rates (Fig. 3c-f).

The results of the univariate Cox regression showed that both the Node-RADS score and the LNM-Station were significantly associated with OS and DFS (Table 2). Multivariate Cox regression analysis, incorporating all CT and clinical variables, demonstrated that LNM-Station was an independent prognostic factor for both OS (HR 1.31[95%CI:1.04–1.64], $p = 0.021$) and DFS (HR 1.29[95%CI:1.02–1.64], $p = 0.036$) (Table 2). The cN stage was also an independent prognostic factor for OS (HR2.70[95%CI:1.11–6.59], $p = 0.029$) and DFS (HR 2.88[95%CI:1.12–7.36], $p = 0.028$) (Table A.2).

The proportional effect of LNM-Station on OS was consistent across subgroup cN1 and cN2 predefined by cN stage (interaction $p > 0.05$, shown in Fig.A.2). Specifically, among patients in the cN1 stage ($p = 0.040$) and cN2 stage ($p = 0.016$), those with multiple metastatic stations demonstrated significantly worse OS compared to those with fewer involved stations. A similar trend was observed in cN3 patients, although the difference did not reach statistical significance ($p = 0.449$).

Performance of pretreatment CT-based prognostic models

The pretreatment CT variables (Node-RADS score, LNM-Station, cT, tumor location and size) were utilized to build the Node-RADS-CT model for predicting OS/DFS (Table A.3). According to multivariate Cox regression, cT4 (OS: HR, 5.03, $p = 0.027$; DFS: HR, 4.36, $p = 0.046$) and multiple LNM-Station (OS: HR, 1.32,

Table 1 Clinicopathological characteristics

Variables	Total ($n=118$)		
Age at diagnosis, Mean ± SD	54.41 ± 11.25	Lauren type, n (%)	
BMI (kg/m^2), M (Q_1, Q_3)	21.72 (19.44, 23.43)	Intestinal	18 (15.25)
Sex, n (%)		Diffuse	72 (61.02)
Male	82 (69.49)	mixed	28(23.72)
Female	36 (30.51)	Differentiation, n (%)	
Smoking, n (%)		Well	2 (1.69)
No	66 (55.93)	Moderate	17 (14.41)
Yes	52 (44.07)	Poor and undifferentiated	99 (83.90)
Diabetes, n (%)		TRG, n(%)	
No	109 (92.37)	0–1	22(18.64)
Yes	9 (7.63)	2–3	96(81.36)
CEA (ng/mL), M (Q_1, Q_3)	2.16 (1.23, 3.37)	ypT stage, n (%)	
CA19-9 (U/mL), M (Q_1, Q_3)	9.48 (3.99, 19.95)	0	9 (7.63)
Tumor location, n (%)		1	11 (9.32)
Cardia	15 (12.71)	2	20 (16.95)
Body	41 (34.75)	3	66 (55.93)
Antrum	59 (50.00)	4	12 (10.17)
Whole	3 (2.54)	ypN stage, n (%)	
Clinical T stage, n (%)		0	39 (33.05)
2	12 (10.17)	1	26 (22.03)
3	25 (21.19)	2	19 (16.10)
4	81 (68.64)	3	34 (28.81)
Clinical N stage, n (%)		Recurrence, n (%)	
0	16 (13.56)	No	57 (48.31)
1	20 (16.95)	Yes	61 (51.69)
2	43 (36.44)	Death, n(%)	
3	39 (33.05)	No	55 (46.61)
		Yes	63 (53.39)

SD: standard deviation, BMI: body mass index, M: median, Q_1: 1st quartile, Q_3: 3st quartile, TRG: tumor regression grade

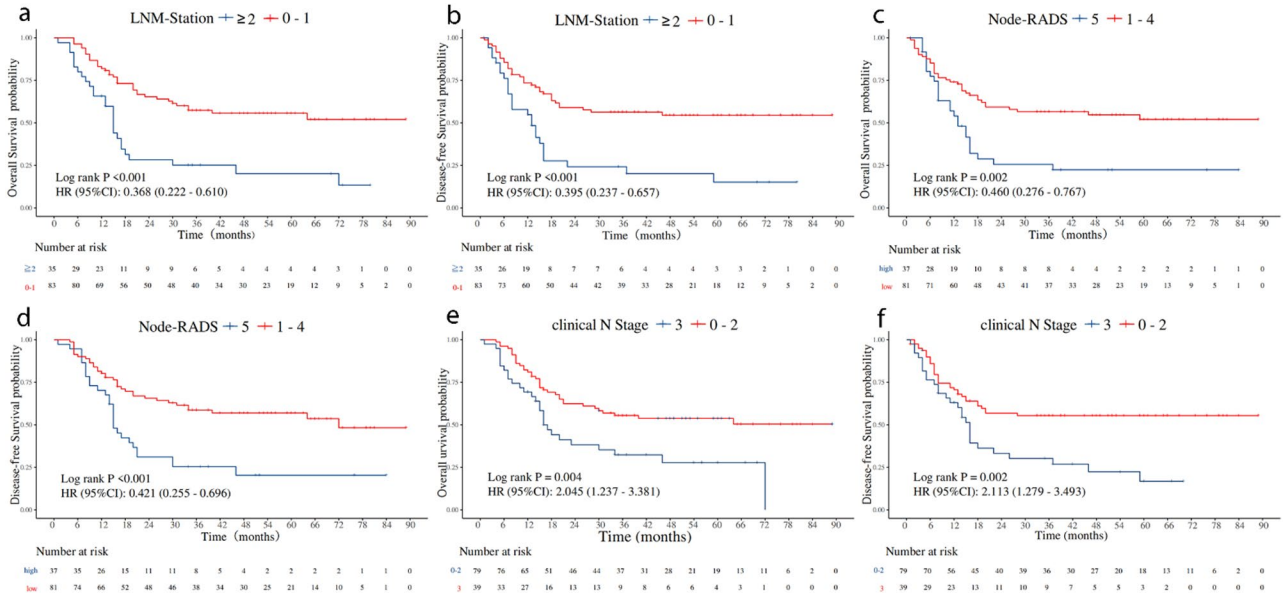

Fig. 3 Kaplan-Meier survival curves. Kaplan-Meier survival curves stratified by LNM-Station (≥ 2 vs. 0–1) for OS (**a**) and DFS (**b**), Node-RADS score (5 vs. 1–4) for OS (**c**) and DFS (**d**), cN (3 vs. 0–2) for OS (**e**) and DFS (**f**). Node-RADS, Node Reporting and Data System; LNM-Station, number of positive lymph node stations; OS, overall survival; DFS, disease-free survival

Table 2 Univariate and multivariate Cox regression analyses for overall survival and disease-free survival

Variables	Overall survival				Disease-free survival			
	Univariate cox regression		Multivariate cox regression		Univariate cox regression		Multivariate cox regression	
	HR (95%CI)	*P*	HR (95%CI)	*P*	HR (95%CI)	*P*	HR (95%CI)	*P*
Tumor Size	1.13 (0.99 ~ 1.28)	0.071			1.20 (1.06 ~ 1.36)	**0.004**	1.11 (0.94 ~ 1.30)	0.214
Tumor Location								
Cardia	1.00 (Reference)				1.00 (Reference)		1.00 (Reference)	
Body	1.11 (0.50 ~ 2.46)	0.806			1.14 (0.52 ~ 2.52)	0.742	1.18 (0.50 ~ 2.83)	0.705
Antrum	0.66 (0.30 ~ 1.45)	0.302			0.62 (0.28 ~ 1.37)	0.239	0.96 (0.40 ~ 2.29)	0.921
Whole	3.14 (0.82 ~ 12.00)	0.094			4.43 (1.15 ~ 17.09)	**0.031**	3.01 (0.65 ~ 13.95)	0.160
LNM-Station	1.51 (1.28 ~ 1.77)	**< 0.001**	1.31 (1.04 ~ 1.64)	**0.021**	1.45 (1.22 ~ 1.71)	**< 0.001**	1.29 (1.02 ~ 1.64)	**0.036**
Node-RADS Score								
1	1.00 (Reference)		1.00 (Reference)		1.00 (Reference)		1.00 (Reference)	
2	2.27 (0.28 ~ 18.51)	0.442	1.46 (0.17 ~ 12.31)	0.730	1.98 (0.24 ~ 16.45)	0.528	1.22 (0.14 ~ 10.72)	0.860
3	2.67 (0.33 ~ 21.36)	0.355	1.46 (0.18 ~ 12.15)	0.726	3.64 (0.47 ~ 28.49)	0.218	1.69 (0.20 ~ 14.27)	0.630
4	4.05 (0.53 ~ 30.88)	0.177	1.57 (0.19 ~ 12.69)	0.671	3.85 (0.50 ~ 29.51)	0.194	1.33 (0.16 ~ 11.24)	0.791
5	9.04 (1.23 ~ 66.68)	**0.031**	2.53 (0.31 ~ 20.78)	0.386	8.95 (1.21 ~ 66.06)	**0.032**	2.26 (0.27 ~ 19.08)	0.454
Clinical T stage								
2	1.00 (Reference)		1.00 (Reference)		1.00 (Reference)		1.00 (Reference)	
3	1.26 (0.24 ~ 6.51)	0.782	1.11 (0.21 ~ 5.86)	0.902	1.22 (0.24 ~ 6.27)	0.815	1.02 (0.19 ~ 5.44)	0.985
4	6.40 (1.55 ~ 26.32)	**0.010**	4.62 (1.10 ~ 19.38)	**0.036**	6.35 (1.54 ~ 26.11)	**0.010**	4.01 (0.94 ~ 17.15)	0.061
CEA	0.86 (0.74 ~ 1.00)	0.057			0.91 (0.80 ~ 1.03)	0.142		
CA19-9	1.01 (1.01 ~ 1.01)	**< 0.001**	1.01 (1.01 ~ 1.01)	**< 0.001**	1.01 (1.01 ~ 1.01)	**< 0.001**	1.01 (1.01 ~ 1.01)	**0.001**
Age at diagnosis	1.00 (0.97 ~ 1.02)	0.821			1.00 (0.98 ~ 1.02)	0.956		
Sex								
Male	1.00 (Reference)				1.00 (Reference)			
Female	1.62 (0.97 ~ 2.70)	0.065			1.55 (0.92 ~ 2.61)	0.096		
BMI	0.95 (0.88 ~ 1.03)	0.250			0.95 (0.88 ~ 1.03)	0.236		
Smoking								
No	1.00 (Reference)				1.00 (Reference)			
Yes	0.68 (0.41 ~ 1.13)	0.133			0.88 (0.53 ~ 1.46)	0.622		
Diabetes								
No	1.00 (Reference)				1.00 (Reference)			
Yes	0.81 (0.30 ~ 2.24)	0.690			0.57 (0.18 ~ 1.82)	0.341		
WBC	0.94 (0.80 ~ 1.09)	0.384			0.94 (0.81 ~ 1.09)	0.433		
Lymphocyte	0.96 (0.71 ~ 1.31)	0.797			1.01 (0.78 ~ 1.32)	0.939		
Platelet	1.00 (1.00 ~ 1.00)	0.901			1.00 (1.00 ~ 1.00)	0.963		
Hemoglobin	0.99 (0.98 ~ 0.99)	0.050			0.99 (0.98 ~ 1.00)	0.093		

HR: hazards ratio, CI: confidence interval, LNM-Station: number of positive lymph node stations, Node-RADS: Node Reporting and Data System, BMI: body mass index, WBC: white blood cell

$p = 0.013$; DFS: HR, 1.32, $p = 0.020$) were independent predictors for poor prognosis.

As a control, the cN-CT models were also constructed for predicting OS/DFS, based on the traditional CT variables (cN, cT, tumor location and size). The cT4 (OS: HR, 6.04, $p = 0.015$; DFS: HR, 5.11, $p = 0.029$) and cN3 (OS: HR, 2.52, $p = 0.042$; DFS: HR, 2.62, $p = 0.042$) were proved independent predictors for poor prognosis, according to multivariate Cox regression (Table A.4).

The C-index of the Node-RADS-CT model for OS exhibited a significant increase compared to the cN-CT model for OS (0.755[95%CI:0.702–0.808] vs. 0.693[95%CI:0.632–0.754], $p = 0.017$), so did the Node-RADS-CT model for DFS compared to the cN-CT model for DFS (0.759[95%CI:0.705–0.814 vs. 0.706[95%CI:0.646–0.766], $p = 0.018$). Furthermore, in terms of the Time-ROC curves for 1-, 3-, 5-year OS and DFS, the Node-RADS-CT model exhibited superior AUC values compared to the cN-CT model (Fig. 4a-b). In addition, the AUC values of the Time-ROC increased over time, suggesting that the Node-RADS-CT model showed better predictive value for the long-term survival outcomes of LAGC.

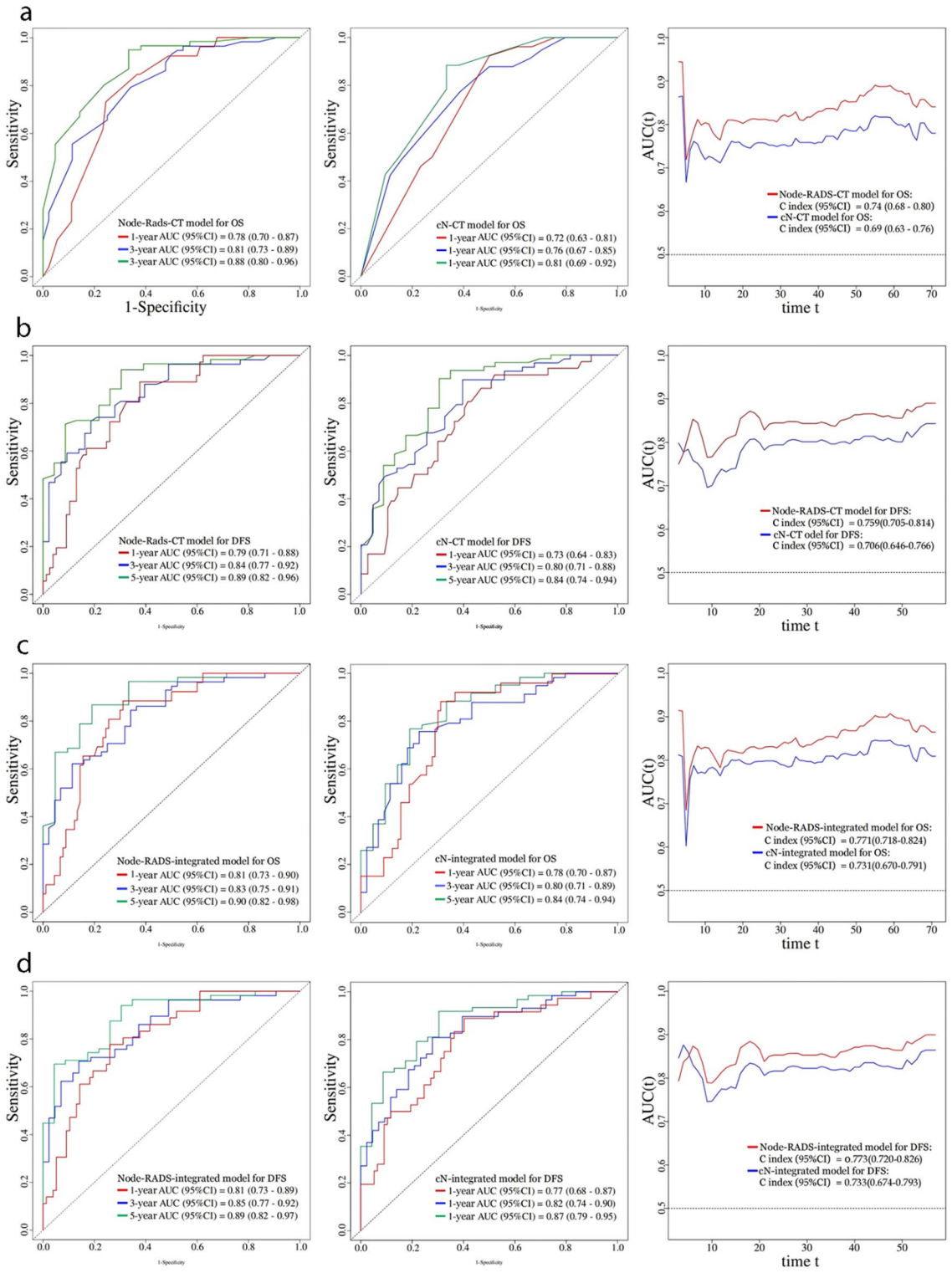

Fig. 4 Time-ROC curves. Time-ROC curves of the Node-RADS-CT and cN-CT models for 1-, 3-, 5-year OS (**a**) and DFS (**b**), Node-RADS-integrated and cN-integrated models for 1-, 3-, 5-year OS (**c**) and DFS (**d**). Time-ROC, Time-dependent receiver-operator characteristic; Node-RADS, Node Reporting and Data System; OS, overall survival; DFS, disease-free survival

Performance of prognostic models integrating pretreatment CT and clinical data

The Node-RADS-integrated models were constructed to predict the OS/DFS, which incorporated the above Node-Rads-CT models and clinical variables before NAC. Multivariate Cox regression revealed that the independent predictors for both OS and DFS were LNM-Station (OS: HR, 1.31[95%CI:1.04–1.64], $p = 0.021$; DFS: HR, 1.29[95%CI:1.02–1.64], $p = 0.036$) and CA19-9 (OS: HR, 1.01[95%CI:1.01–1.01], $p < 0.001$; DFS: HR, 1.01[95%CI:1.01–1.01], $p = 0.001$)(Table 2). In addition, cT4 (HR: 4.62[CI:1.10-19.38], $p = 0.036$) was significantly related with worse OS (Table 2).

As a contrast, the cN-integrated models were established, which incorporated the above cN-CT models and clinical variables before NAC. The tumor location was associated with DFS ($p = 0.048$). The cT4, cN3 stage and high CA19-9 were significantly associated with worse OS and DFS (all $p < 0.05$) (Table A.2).

Notably, the C-index values of the Node-RADS-integrated models were also higher than those of the cN-integrated models for OS (0.771[95%CI:0.718–0.824] vs. 0.731[95%CI:0.670–0.791], $p = 0.091$) and DFS (0.773[95%CI:0.720–0.826] vs. 0.733[95%CI:0.674–0.793], $p = 0.053$), which nearly reached statistical significance. The AUC values of 1-, 3-, 5-year Time-ROC of the Node-RADS-integrated models were all higher than those of the cN models. The AUC values also increased over time (Fig. 4c-d).

The nomograms of the Node-RADS based models for OS and DFS are depicted in Fig. 5a-d. The calibration curves demonstrated a high degree of concordance between the Node-RADS based models and actual observations at 1, 3 and 5 years (Fig. 5e-h). The DCA curves suggested that Node-RADS-based model for OS can obtain a greater net benefit than the cN model (Fig. 5i-l).

Moreover, we quantified the improvement in survival prediction accuracy for the Node-RADS-integrated models versus the cN-integrated models. The NRI for OS was 0.379 (95%CI:0.051–0.581, $p = 0.04$) and the NRI for DFS was 0.364 (95%CI:0.014–0.633, $p = 0.04$). The IDI for OS was 0.103 (95%CI:0.008–0.206, $p = 0.02$) and IDI for DFS was 0.107 (95%CI:0.016–0.221, $p = 0.01$).

Relations of Post-NAC pathological status to pretreatment LN characteristics in CT and prognosis

The detailed pathological conditions after NAC are shown in Table A.5–7. The pretreatment Node-RADS score, LNM-Station and cN stage were significantly associated with ypN and ypLNR (all $p < 0.001$). The Node-RADS score also showed a positive correlation with tumor regression grade (TRG) ($p = 0.035$). The ypN, ypT stage, ypLNR and TRG were significantly associated with both OS and DFS (all $p < 0.05$), according to the results of univariate Cox regression (Table A.8).

Performance of Post-NAC pathological prognostic models

The pathological prognostic models were constructed based on the post-NAC pathological characteristics. After NAC, 22 patients (18.6%) achieved TRG 0–2 and 96 patients (81.36%) achieved TRG 3. Univariate cox regression demonstrated that ypT, ypN, ypLNR and TRG were significantly associated with both OS and DFS. Multivariate Cox regression revealed TRG 3 and ypN 2–3 stage were independent predictors for poor OS and DFS (all $p < 0.05$, Table A.8). The C-index values (OS: 0.745[95%CI:0.683–0.807], DFS: 0.746[95%CI:0.688–0.805]) of pathological prognostic models were slightly higher than those of two cN based models, whereas slightly lower than those of two Node-RADS-based models, without significant statistical differences (all $p > 0.05$).

Discussion

Gastric cancer has high mortality and recurrence rate, even with the survival benefit brought by NAC [1]. LN metastasis significantly contributes to a poor prognosis in LAGC [11, 12]. We retrospectively assessed the correlations of pretreatment Node-RADS-related CT characteristics with post-NAC pathological, OS and DFS status of LAGC. Subsequently, we developed Node-RADS-CT prognostic models based on pre-NAC CT to compare with conventional cN-CT models. Additionally, Node-RADS-integrated prognostic models incorporating imaging and clinical variables were also developed in comparison with the conventional cN-integrated models. Our results revealed that the baseline Node-RADS-related CT characteristics were significantly correlated with post-NAC pathological and prognosis of LAGC. The Node-RADS-CT models exhibited better discriminative performance compared to the cN-CT model. After incorporating clinical variables, the Node-RADS-integrated models still showed better prognostic performance than the cN-integrated models.

The Reporting and Data Systems have been successfully applied in the staging and predicting prognosis for malignancies [31–33]. The Node-RADS was proposed to standardize the assessment of LNs, which has brought improved diagnostic performance for LNs assessment in different cancers [16, 23–28, 34]. To the best of our knowledge, there are currently no reports on utilizing Node-RADS to predict the prognosis of malignant tumors, and the present study might be the first one. In this study, Kaplan-Meier curves and Cox survival analysis revealed that pretreatment Node-RADS-related CT indicators (Node-RADS score and LNM-Station) were associated with OS and DFS in LAGC patients. Lower Node-RADS score and LNM-Station indicate better

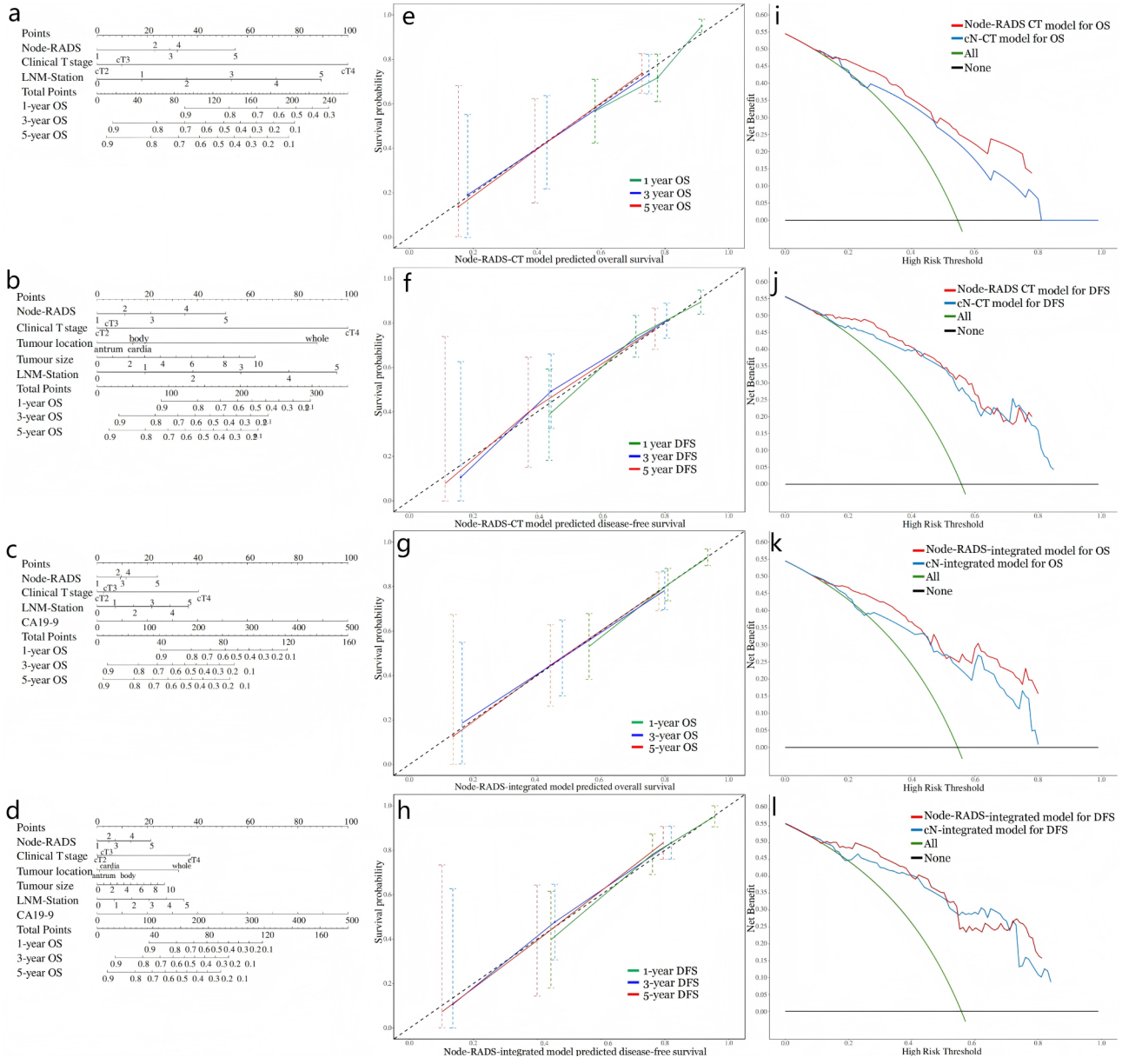

Fig. 5 Nomogram, calibration curves and DCA curves for Node-RADS based models. The nomogram of the Node-RADS-CT model for OS (**a**) and DFS (**b**), and of the Node-RADS-integrated model for OS (**c**) and DFS (**d**). The calibration curves at 1, 3 and 5 years of the Node-RADS-CT model for OS (**e**) and DFS (**f**), and of the Node-RADS-integrated model for OS (**g**) and DFS (**h**). The DCA curves of the Node-RADS-CT model for OS (**i**) and DFS (**j**), and of the Node-RADS-integrated model for OS (**k**) and DFS (**l**). DCA, decision curve analysis; Node-RADS, Node Reporting and Data System; OS, overall survival; DFS, disease-free survival

survival outcomes. This finding could offer novel perspectives for extending the application of Node-RADS in prognostic studies of malignant tumors, including LAGC.

In the present study, a Node-RADS score of 5 was associated with poorer prognosis in LAGC. The Node-RADS system combines LN size and morphological abnormalities (texture, border, shape), with their contributions being cumulative. In other words, the larger the LN and the greater the number of morphological abnormalities, the higher the score, indicating a greater likelihood of malignancy. A score of 5 is the highest in the Node-RADS, indicating that the LN has the most morphological abnormalities and/or a larger size. Reportedly, the larger size, necrosis, spherical shape and irregular border of LN typically indicated worse tumor progression and result in poorer survival outcomes [17–20]. In terms of LAGC, these factors may partially reflect higher aggressiveness or a more advanced stage, which correspondingly suggests a poorer NAC therapeutic

effect and subsequent poorer prognosis. This interpretation can be partially confirmed by our observations that the Node-RADS score is positively correlated with ypN, ypLNR, and TRG, indicating more tumor residue after NAC. Meanwhile, ypN, ypLNR and TRG were significantly associated with both OS and DFS, which is in line with previous findings that these factors act as important prognostic indicators for gastric cancer [11, 35–37]. Consequently, it is reasonable and feasible for the pretreatment Node-RADS score to serve as an effective prognostic indicator. Radiologists could incorporate Node-RADS scoring alongside traditional staging methods to provide a more nuanced assessment of lymph node involvement.

Similar to Node-RADS score, LNM-Station of ≥ 2, indicating multiple positive LN stations, was also associated with poor survival outcome for LAGC patients in this study. The presence of multiple positive stations suggests that metastatic LNs have spread more extensively, which typically signifies advanced tumor progression. Previous studies have shown that the number of LN stations involved is linked to prognosis in non-small cell lung cancer [21, 22], which is similar to our study. Unfortunately, few studies have focused on the prognostic value of the number of LN stations involved in LAGC. In this study, LNM-Station was strongly associated with ypN and ypLNR, which indicates more tumor residue after NAC. As demonstrated above, both ypLNR and ypN have been established as prognostic indicators in our study, consistent with previous reports [11, 35, 37]. In light of these findings, it is reasonable to conclude that pretreatment LNM-Station can sever as a potential prognostic indicator for LAGC.

Interestingly, regarding the two Node-RADS-related indicators in our study, only LNM-Station was ultimately included as an independent predictor in both the CT-based model and the model that integrated clinical and CT data, regardless of whether predicting OS or DFS, whereas Node-RADS score was not. This finding suggests that LNM-Station might be a better CT indicator for LAGC prognosis than the Node-RADS score.

The AJCC cN staging system which classifies gastric cancer based on the number of suspicious metastatic LNs, serves as an important prognostic factor. However, clinical observations reveal substantial survival heterogeneity among patients within the same cN stage. Our analysis demonstrated that cN1 and cN2 patients with multiple metastatic stations had significantly worse OS than those with fewer involved stations. This finding suggests that the LNM-Station parameter serves as a valuable indicator for differentiating prognostic outcomes among patients within the same cN1/2 staging category. These results indicate that LNM-Station may represent a clinically valuable supplementary prognostic stratification tool for gastric cancer patients in cN1 or cN2 stage, potentially enhancing the precision of current staging systems. However, the current evidence remains preliminary and warrants further validation through rigorously designed multicenter studies with larger patient cohorts, prospective and multicenter data collection.

In this study, cN stage was also an independent predictor for OS/DFS in LAGC, consistent with previous report [12]. Therefore, we constructed two CT-based prediction models based on pretreatment CT characteristics: the Node-RADS-CT and cN-CT models. The only difference between the two models in terms of incorporated predictive variables was that the former included Node-RADS-related CT indicators, while the latter included cN. The same situation also applied to the two integrated models combining clinical and CT data, namely the Node-RADS-integrated and cN-integrated models. In this study, both the CT-based and the integrated models, those containing Node-RADS-related CT indicators exhibited higher predictive efficiency than those incorporating cN data.

Considering the near-significant differences in C-index between Node-RADS-integrated and cN-integrated prognostic models ($p = 0.091$ and 0.053), we subsequently conducted NRI and IDI analyses. Although C-index is commonly used to measure model discrimination, it is not sensitive to slight changes in absolute risk estimates, particularly when the initial C-index is already high [38]. In this study, the initial C-index was 0.731 for OS and 0.733 for DFS, so replacing only one predictor (cN) might not substantially affect C-index. To address this, we introduced two additional metrics, NRI and IDI, which are rapidly adopted to quantify the added value of a new biomarker to an existing test [39]. The NRI and IDI comparisons between Node-RADS-integrated and cN-integrated models showed excellent performance in predicting OS and DFS (all $p < 0.05$), indicating that Node-RADS-related indicators significantly enhanced the prognostic and discriminatory capabilities of the initial model.

Notably, compared to pathological models, the Node-RADS-integrated models exhibited a slightly higher C-index, suggesting that for predicting prognosis in LAGC, the baseline Node-RADS–integrated models offer predictive performance that is at least comparable to, possibly better than, the pathological models. Therefore, it is expected to help us identify LAGC patients with a poor prognosis before the initiation of NAC and provide them with more appropriate and aggressive interventions, such as radiotherapy or immunotherapy, to improve their survival rate.

This study has several limitations that should be acknowledged. First, the retrospective design may introduce inherent biases in the findings. To address this

limitation, we plan to conduct future prospective studies with an expanded cohort and implement propensity score matching to reduce potential selection bias. Second, the single-center design may limit the generalizability and statistical power of our findings. Future multicenter studies with expanded cohorts and external validation are needed to enhance the robustness and clinical applicability of these results. Third, unresectable gastric cancer patients with only chemotherapy or palliative treatment were not included, which may limit the generalizability of this study's findings. Survival in unresectable gastric cancer patients should be investigated in the future study. Finally, our study did not explore the correlation between Node-RADS and signet ring cell (SRC) proportion in G). Recent evidence indicates that SRC percentage may significantly impact prognosis [40]. In our next prospective study, we will evaluate SRC percentage to further assess the prognostic value of Node-RADS.

In conclusion, the Node-RADS score and number of positive LNs stations were effective prognostic indicators for LAGC. In prognosis prediction of LAGC, the baseline Node-RADS-based models can offer superior predictive performance compared to the cN-based models. These Node-RADS-based models show potential for identifying patients at high risk for poor outcomes, allowing for timely intervention and more focused monitoring in clinical practice.

Abbreviations

LAGC	Locally advanced gastric cancer
NAC	Neoadjuvant chemotherapy
OS	Overall survival
TNM	Tumor-node-metastasis
LN	Lymph node
Node-RADS	Node Reporting and Data System 1.0
NCCN	National Comprehensive Cancer Network
CSCO	Chinese Society of Clinical Oncology
TRG	Tumor regression grade
LNR	Lymph node ratio
DFS	Disease-free survival
ICC	Intraclass correlation coefficient
ROC	Receiver-operator characteristic
C-Index	Consistency index
Time-ROC	Time-dependent receiver-operator characteristic
NRI	Net reclassification improvement
IDI	Integrated discrimination improvement
SRC	Signet ring cell

Supplementary Information

The online version contains supplementary material available at https://doi.org/10.1186/s12885-025-14032-z.

Supplementary Material 1

Acknowledgements
Not applicable.

Author contributions
All authors contributed to the study conception and design. Material preparation, data collection and analysis were performed by Y.S., L.W., H.X. and L.C. The first draft of the manuscript was written by Y.S. and X.P.Y. All authors commented on previous versions of the manuscript. All authors read and approved the final manuscript.

Funding
This research did not receive any specific grant from funding agencies in the public, commercial, or not-for-profit sectors.

Data availability
The datasets used during the current study are available from the corresponding author on reasonable request.

Declarations

Ethics approval and consent to participate
All procedures followed were in accordance with the ethical standards of the responsible committee on human experimentation (institutional and national) and with the Helsinki Declaration of 1964 and later versions. This retrospective study was approved by the Ethics Committee of Hunan Cancer Hospital (NO. KT2024524).

Consent for publication
Not applicable.

Competing interests
The authors declare no competing interests.

Author details
[1]Department of Diagnostic Radiology, The Affiliated Cancer Hospital of Xiangya School of Medicine, Central South University/Hunan Cancer Hospital, Changsha, China
[2]Graduate Collaborative Training Base of Hunan Cancer Hospital, Hengyang Medical School, University of South China, Changsha, China
[3]Department of Radiotherapy Technology, The Affiliated Cancer Hospital of Xiangya School of Medicine, Central South University/Hunan Cancer Hospital, Changsha, China
[4]Norman Bethune Health Science Center of Jilin University, Changsha, China
[5]Department of Hepatobiliary and Intestinal Surgery, The Affiliated Cancer Hospital of Xiangya School of Medicine, Central South University/Hunan Cancer Hospital, Changsha, China
[6]Department of Gastroduodenal and Pancreatic Surgery, The Affiliated Cancer Hospital of Xiangya School of Medicine, Central South University/Hunan Cancer Hospital, Changsha, China

Received: 13 February 2025 / Accepted: 27 March 2025
Published online: 02 April 2025

References

1. Bray F, Laversanne M, Sung H, Ferlay J, Siegel RL, Soerjomataram I, Jemal A. Global cancer statistics 2022: GLOBOCAN estimates of incidence and mortality worldwide for 36 cancers in 185 countries. CA Cancer J Clin. 2024;74(3):229–63.
2. Badgwell B. Multimodality therapy of localized gastric adenocarcinoma. J Natl Compr Canc Netw. 2016;14(10):1321–7.
3. Sato Y, Mizusawa J, Katayama H, Nakamura K, Fukagawa T, Katai H, Haruta S, Yamada M, Takagi M, Tamura S, et al. Diagnosis of invasion depth in resectable advanced gastric cancer for neoadjuvant chemotherapy: an exploratory analysis of Japan clinical oncology group study: JCOG1302A. Eur J Surg Oncol. 2020;46(6):1074–9.
4. Cunningham D, Allum WH, Stenning SP, Thompson JN, Van de Velde CJ, Nicolson M, Scarffe JH, Lofts FJ, Falk SJ, Iveson TJ, et al. Perioperative chemotherapy versus surgery alone for resectable gastroesophageal cancer. N Engl J Med. 2006;355(1):11–20.
5. Rawla P, Barsouk A. Epidemiology of gastric cancer: global trends, risk factors and prevention. Prz Gastroenterol. 2019;14(1):26–38.
6. Liu D, Lu M, Li J, Yang Z, Feng Q, Zhou M, Zhang Z, Shen L. The patterns and timing of recurrence after curative resection for gastric cancer in China. World J Surg Oncol. 2016;14(1):305.

7. Yang HK, Ji J, Han SU, Terashima M, Li G, Kim HH, Law S, Shabbir A, Song KY, Hyung WJ, et al. Extensive peritoneal lavage with saline after curative gastrectomy for gastric cancer (EXPEL): a multicentre randomised controlled trial. Lancet Gastroenterol Hepatol. 2021;6(2):120–7.
8. Pietrantonio F, Randon G, Di Bartolomeo M, Luciani A, Chao J, Smyth EC, Petrelli F. Predictive role of microsatellite instability for PD-1 Blockade in patients with advanced gastric cancer: a meta-analysis of randomized clinical trials. ESMO Open. 2021;6(1):100036.
9. Zheng H, Zheng Q, Jiang M, Chen D, Han C, Yi J, Ai Y, Yan J, Jin X. Evaluation the benefits of additional radiotherapy for gastric cancer patients after D2 resection using CT based radiomics. Radiol Med. 2023;128(6):679–88.
10. Badgwell B, Blum M, Elimova E, Estrella J, Chiang YJ, Das P, Mansfield P, Ajani J. Frequency of resection after preoperative chemotherapy or chemoradiotherapy for gastric adenocarcinoma. Ann Surg Oncol. 2016;23(6):1948–55.
11. Ji X, Bu ZD, Yan Y, Li ZY, Wu AW, Zhang LH, Zhang J, Wu XJ, Zong XL, Li SX, et al. The 8th edition of the American joint committee on cancer tumor-node-metastasis staging system for gastric cancer is superior to the 7th edition: results from a Chinese mono-institutional study of 1663 patients. Gastric Cancer: Official J Int Gastric Cancer Association Japanese Gastric Cancer Association. 2018;21(4):643–52.
12. Bando E, Makuuchi R, Tokunaga M, Tanizawa Y, Kawamura T, Terashima M. Impact of clinical tumor-node-metastasis staging on survival in gastric carcinoma patients receiving surgery. Gastric Cancer: Official J Int Gastric Cancer Association Japanese Gastric Cancer Association. 2017;20(3):448–56.
13. Son T, Sun J, Choi S, Cho M, Kwon IG, Kim HI, Cheong JH, Choi SH, Noh SH, Woo Y, et al. Multi-institutional validation of the 8th AJCC TNM staging system for gastric cancer: analysis of survival data from high-volume Eastern centers and the SEER database. J Surg Oncol. 2019;120(4):676–84.
14. In H, Solsky I, Palis B, Langdon-Embry M, Ajani J, Sano T. Validation of the 8th edition of the AJCC TNM staging system for gastric cancer using the National cancer database. Ann Surg Oncol. 2017;24(12):3683–91.
15. Bando E, Makuuchi R, Irino T, Tanizawa Y, Kawamura T, Terashima M. Validation of the prognostic impact of the new tumor-node-metastasis clinical staging in patients with gastric cancer. Gastric Cancer. 2019;22(1):123–9.
16. Loch FN, Beyer K, Kreis ME, Kamphues C, Rayya W, Schineis C, Jahn J, Tronser M, Elsholtz FHJ, Hamm B, et al. Diagnostic performance of node reporting and data system (Node-RADS) for regional lymph node staging of gastric cancer by CT. Eur Radiol. 2024;34(5):3183–93.
17. Sugimura K, Miyata H, Kanemura T, Takeoka T, Sugase T, Yamamoto M, Shinnno N, Hara H, Omori T, Motoori M, et al. Clinical impact of metastatic lymph node size on therapeutic effect and prognosis in patients with esophageal squamous cell carcinoma who underwent preoperative chemotherapy followed by esophagectomy. Ann Surg Oncol. 2023;30(7):4193–202.
18. Fang Q, Zhang X, Dai L, Luo R, Yuan J. Association between factor of Parotid lymph node and prognosis in Parotid cancer. Eur J Surg Oncol. 2023;49(8):1405–10.
19. Rollvén E, Blomqvist L, Öistämö E, Hjern F, Csanaky G, Abraham-Nordling M. Morphological predictors for lymph node metastases on computed tomography in colon cancer. Abdom Radiol (New York). 2019;44(5):1712–21.
20. Li J, Zhao Q, Zhang Y, Li H, Ruan G, Liu L, Yan Y, Cui C. Prognostic value of quantitative cervical nodal necrosis burden on MRI in nasopharyngeal carcinoma and its role as a stratification marker for induction chemotherapy. Eur Radiol. 2022;32(11):7710–21.
21. Ichinose Y, Kato H, Koike T, Tsuchiya R, Fujisawa T, Shimizu N, Watanabe Y, Mitsudomi T, Yoshimura M, Tsuboi M. Completely resected stage IIIA non-small cell lung cancer: the significance of primary tumor location and N2 station. J Thorac Cardiovasc Surg. 2001;122(4):803–8.
22. Sayar A, Turna A, Kiliçgün A, Solak O, Urer N, Gürses A. Prognostic significance of surgical-pathologic multiple-station N1 disease in non-small cell carcinoma of the lung. Eur J Cardiothorac Surg. 2004;25(3):434–8.
23. Elsholtz FHJ, Asbach P, Haas M, Becker M, Beets-Tan RGH, Thoeny HC, Padhani AR, Hamm B. Introducing the node reporting and data system 1.0 (Node-RADS): a concept for standardized assessment of lymph nodes in cancer. Eur Radiol. 2021;31(8):6116–24.
24. Maggialetti N, Greco CN, Lucarelli NM, Morelli C, Cianci V, Sasso S, Rubini D, Scardapane A, Stabile Ianora AA. Applications of new radiological scores: the Node-rads in colon cancer staging. Radiol Med. 2023;128(11):1287–95.
25. Leonhardi J, Sabanov A, Schnarkowski B, Hoehn AK, Sucher R, Seehofer D, Denecke T, Meyer HJ. CT texture analysis and Node-RADS CT score of lymph nodes in patients with Perihilar cholangiocarcinoma. Anticancer Res. 2023;43(11):5089–97.
26. Meyer HJ, Schnarkowski B, Pappisch J, Kerkhoff T, Wirtz H, Höhn AK, Krämer S, Denecke T, Leonhardi J, Frille A. CT texture analysis and node-RADS CT score of mediastinal lymph nodes - diagnostic performance in lung cancer patients. Cancer Imaging. 2022;22(1):75.
27. Leonardo C, Flammia RS, Lucciola S, Proietti F, Pecoraro M, Bucca B, Licari LC, Borrelli A, Bologna E, Landini N et al. Performance of Node-RADS scoring system for a standardized assessment of regional lymph nodes in bladder cancer patients. Cancers (Basel) 2023, 15(3).
28. Wu Q, Lou J, Liu J, Dong L, Wu Q, Wu Y, Yu X, Wang M. Performance of node reporting and data system (node-RADS): a preliminary study in cervical cancer. BMC Med Imaging. 2024;24(1):28.
29. Ajani JA, D'Amico TA, Bentrem DJ, Chao J, Cooke D, Corvera C, Das P, Enzinger PC, Enzler T, Fanta P, et al. Gastric cancer, version 2.2022, NCCN clinical practice guidelines in oncology. J Natl Compr Canc Netw. 2022;20(2):167–92.
30. Wang FH, Zhang XT, Tang L, Wu Q, Cai MY, Li YF, Qu XJ, Qiu H, Zhang YJ, Ying JE, et al. The Chinese society of clinical oncology (CSCO): clinical guidelines for the diagnosis and treatment of gastric cancer, 2023. Cancer Commun (London England). 2024;44(1):127–72.
31. Spak DA, Plaxco JS, Santiago L, Dryden MJ, Dogan BE. BI-RADS(®) fifth edition: A summary of changes. Diagn Interv Imaging. 2017;98(3):179–90.
32. Turkbey B. AS Purysko 2023 PI-RADS: where next?? Radiology 307 5 e223128.
33. Tessler FN, Middleton WD, Grant EG, Hoang JK, Berland LL, Teefey SA, Cronan JJ, Beland MD, Desser TS, Frates MC, et al. ACR thyroid imaging, reporting and data system (TI-RADS): white paper of the ACR TI-RADS committee. J Am Coll Radiol. 2017;14(5):587–95.
34. Niu Y, Wen L, Yang Y, Zhang Y, Fu Y, Lu Q, et al. Diagnostic performance of Node Reporting and Data System (Node-RADS) for assessing mesorectal lymph node in rectal cancer by CT. BMC Cancer. 2024;24:716.
35. Kano K, Yamada T, Yamamoto K, Komori K, Watanabe H, Hara K, Shimoda Y, Maezawa Y, Fujikawa H, Aoyama T, et al. Association between lymph node ratio and survival in patients with pathological stage II/III gastric cancer. Ann Surg Oncol. 2020;27(11):4235–47.
36. Westerhoff M, Osecky M, Langer R. Varying practices in tumor regression grading of Gastrointestinal carcinomas after neoadjuvant therapy: results of an international survey. Mod Pathology: Official J United States Can Acad Pathol Inc. 2020;33(4):676–89.
37. Zhu J, Xue Z, Zhang S, Guo X, Zhai L, Shang S, Zhang Y, Lu H. Integrated analysis of the prognostic role of the lymph node ratio in node-positive gastric cancer: A meta-analysis. Int J Surg. 2018;57:76–83.
38. Alba AC, Agoritsas T, Walsh M, Hanna S, Iorio A, Devereaux PJ, McGinn T, Guyatt G. Discrimination and calibration of clinical prediction models: users' guides to the medical literature. JAMA. 2017;318(14):1377–84.
39. Pencina MJ, D'Agostino RB, Sr., D'Agostino RB Jr., Vasan RS. Evaluating the added predictive ability of a new marker: from area under the ROC curve to reclassification and beyond. Stat Med. 2008;27(2):157–72. discussion 207– 112.
40. Marano L, Ambrosio MR, Resca L, Carbone L, Carpineto Samorani O, Petrioli R, Savelli V, Costantini M, Malaspina L, Polom K, et al. The percentage of signet ring cells is inversely related to aggressive behavior and poor prognosis in Mixed-Type gastric cancer. Front Oncol. 2022;12:897218.

Publisher's note